Received: 24 January 2020 | Revised: 8 August 2020 | Accepted: 27 August 2020

DOI: 10.1096/fj.202000177R

RESEARCH ARTICLE

THE FASEB JOURNAL

CD163 deficiency increases foam cell formation and plaque progression in atherosclerotic mice

Carmen Gutiérrez-Muñoz[1] | Nerea Méndez-Barbero[1,2] | Pia Svendsen[3] | Cristina Sastre[4] | Valvanera Fernández-Laso[1,2] | Patricia Quesada[1] | Jesús Egido[5,6] | Joan C. Escolá-Gil[6,7] | Jose L. Martín-Ventura[1,2] | Soren K. Moestrup[8,9] | Luis M. Blanco-Colio[1,2]

[1]Vascular Research Laboratory, IIS-Fundación Jiménez Díaz University Hospital, Madrid, Spain

[2]Centro de Investigación Biomédica en Red de Enfermedades Cardiovasculares (CIBERCV), Madrid, Spain

[3]Department of Clinical Medicine, Aarhus University Hospital, Aarhus, Denmark

[4]Center for Genomic Medicine, Massachusetts General Hospital, Boston, MA, USA

[5]Renal, Vascular and Diabetes Research Laboratory, IIS-Fundación Jiménez Díaz, Madrid, Spain

[6]Centro de Investigación Biomédica en Red de Diabetes y Enfermedades Metabólicas (CIBERDEM), Madrid, Spain

[7]Institut d'Investigacions Biomèdiques (IIB) Sant Pau, Barcelona, Spain

[8]Department of Molecular Medicine, University of Southern Denmark, Oddense, Denmark

[9]Department of Biomedicine, Aarhus University, Aarhus, Denmark

Correspondence

Abstract

Atherosclerosis is an inflammatory disease characterized by the accumulation of macrophages in the vessel wall. Macrophages depend on their polarization to exert either pro-inflammatory or anti-inflammatory effects. Macrophages of the anti-inflammatory phenotype express high levels of CD163, a scavenger receptor for the hemoglobin-haptoglobin complex. CD163 can also bind to the pro-inflammatory cytokine TWEAK. Using *ApoE*-deficient or *ApoE/CD163* double-deficient mice we aim to investigate the involvement of CD163 in atherosclerosis development and its capacity to neutralize the TWEAK actions. *ApoE/CD163* double-deficient mice displayed a more unstable plaque phenotype characterized by an increased lipid and macrophage content, plaque size, and pro-inflammatory cytokine expression. In vitro experiments demonstrated that the absence of CD163 in M2-type macrophages-induced foam cell formation through upregulation of CD36 expression. Moreover, exogenous TWEAK administration increased atherosclerotic lesion size, lipids, and macrophages content in $ApoE^{-/-}/CD163^{-/-}$ compared with $ApoE^{-/-}/CD163^{+/+}$ mice. Treatment with recombinant CD163 was able to neutralize the proatherogenic effects of TWEAK in *ApoE/CD163 double*-deficient mice. Recombinant CD163 abolished the pro-inflammatory actions of TWEAK on vascular smooth muscle cells, decreasing NF-kB activation, cytokines and metalloproteinases expression, and macrophages migration. In conclusion, CD163-expressing macrophages serve as a protective mechanism to

Abbreviations: ABCA1, ATP-binding cassette subfamily; ABCG1, ATP-binding cassette subfamily G member 1; ADAM17, ADAM metallopeptidase domain 17; $ApoE^{-/-}$, apolipoprotein E-deficient mice; Arg1, arginase 1; BCA, brachiocephalic arteries; CCL2, chemokine ligand 2; CCL5, chemokine ligand 5; CD36, cluster of differentiation 36; CD68, cluster of differentiation 68; CD163, 130nonbreakingspacekDa member of the scavenger receptor cysteine rich (SRCR) family; Fn14, fibroblast growth factor-inducible 14; ICAM-1, intercellular adhesion molecule 1; IL-4, interleukin 4; IL-10, interleukin 10; IL-13, interleukin 13; LDH, lactate dehydrogenase; LXR, liver X receptor; MMP-2, matrix metallopeptidase 2; MMP-9, matrix metallopeptidase 9; NF-kB, nuclear factor-kB; Nos2, nitric oxide synthase 2; ORO, Oil Red O; ox-LDL, oxidized low-density lipoproteins; rCD, recombinant 130nonbreakingspacekDa member of the scavenger receptor cysteine rich (SRCR) family; rTW, recombinant soluble tumor necrosis factor-like weak inducer of apoptosis; SR-A, scavenger receptor A; TWEAK, tumor necrosis factor-like weak inducer of apoptosis; VSMCs, vascular smooth muscle cells.

Carmen Gutiérrez-Muñoz and Nerea Méndez-Barbero contributed equally to this work.

Luis M. Blanco-Colio, Vascular Research Laboratory, IIS-Fundación Jiménez Díaz University Hospital, Av. Reyes Católicos 2, 28040, Madrid, Spain.
Email: lblanco@fjd.es

Funding information
MINECO | Instituto de Salud Carlos III (ISCIII), Grant/Award Number: PI16/01419 and PI19/00128

prevent the deleterious effects of TWEAK on atherosclerotic plaque development and progression.

KEYWORDS
atherosclerosis, CD163, inflammation, TWEAK

1 | INTRODUCTION

Atherosclerosis is a lipid-driven inflammatory disease characterized by monocyte recruitment and differentiation to macrophages/foam cells.[1] During the early stages of atherosclerosis, oxidized low-density lipoproteins (ox-LDL) accumulated in the intima, induce the activation of both endothelial cells and vascular smooth muscle cells (VSMCs), leading to the expression and secretion of several pro-inflammatory cytokines, chemokines, and adhesion molecules that recruit monocytes within the arterial wall. Within the intima, monocytes differentiate into the macrophages to remove ox-LDL. Macrophages are heterogeneous immune cells that respond to the pathophysiological signals such as lipopolysaccharide and interferon-γ to form pro-inflammatory M1 phenotype or to IL-4 and IL-13 leading to anti-inflammatory M2 phenotype.[2] Whereas the M1-type macrophages seem to have direct effect in pathogen killing, M2-type macrophage express high levels of scavenging molecules and anti-inflammatory cytokines, promoting tissue remodeling.[3] However, M1/M2 nomenclature is a simplification of a continuum of complex macrophage phenotypes.

M2-type macrophages express high levels of CD163, a member of the scavenger receptor cysteine rich family.[4] CD163 was identified as an endocytic receptor for removal of hemoglobin:haptoglobin (Hb:Hp) complexes to avoid toxic effects of the oxidant Hb.[5] Scavenging of Hb:Hp complexes by CD163 is part of an adaptive process, linked to secretion of the anti-inflammatory cytokine interleukin-10 and elevation of heme oxygene-1.[6] Shedding of the extracellular domain of CD163 from macrophages by ADAM17 generates a soluble form (sCD163) that is a normal constituent of plasma.[7] CD163 is considered an anti-inflammatory molecule involved in the resolution of inflammation since pro-inflammatory stimuli reduce its expression.[8,9] Decreased expression of CD163 on peripheral blood mononuclear cells has been observed in patients with a specific Hp genotype (Hp 2 to 2), which is associated with an increased risk of cardiovascular disease.[10] In addition, CD163 expression is associated to areas with inflammation in injured tissues.[6] However, it was reported that the presence of CD163-expressing macrophages promotes plaque angiogenesis and vascular permeability in human atherosclerosis.[11] Nevertheless, the direct role of CD163 in the development of atherosclerotic plaques deserves further studies.

CD163 is also a scavenger receptor for tumor necrosis factor-like weak inducer of apoptosis (TWEAK; *Tnfsf12*).[12] TWEAK and its soluble form are mainly expressed and secreted by inflammatory leukocytes.[13] TWEAK acts by binding to its sole functional receptor fibroblast growth factor-inducible 14 (Fn14; *Tnfrsf12a*) that is linked to several intracellular and inflammatory signaling pathways.[14] The signaling induced by TNF superfamily receptors involves the presence of death domains in their cytoplasmic tail. However, the Fn14 cytoplasmic tail is too short to have a death domain, but it contains a TNF receptor-associated factor (TRAF)-binding site that could be potentially phosphorylated to induce TRAF-binding and subsequent transmission of TWEAK signaling.[15] TWEAK trimerizes and binds to Fn14 monomers, promoting receptor trimerization and signal transduction.[15] Both, TWEAK and Fn14 are closely related in humans and mice, being that their homology is higher than 90%.[16] This detail is of importance since TWEAK does not cross-react with any other members of the TNF or TNFR superfamilies, being its interaction specific for Fn14.

TWEAK/Fn14 axis participates in several steps related to atherosclerotic plaque development and progression such as endothelial dysfunction, inflammation, proliferation, and thrombosis.[17-19] In fact, while recombinant TWEAK injection aggravates vascular lesion,[20] TWEAK deficiency as well as Fn14-Fc or anti-TWEAK antibody treatment display reduced atherosclerotic lesion size and increased plaque stability in *ApoE*-deficient mice.[21,22] However, little is known about the biological mechanisms regulating TWEAK bioavailability and the downstream pathways by which TWEAK might participate in atherosclerotic progression.

In the present study, we have now investigated how CD163 deficiency affects TWEAK levels and atherosclerosis in mice to further investigate the role of CD163 during atherosclerosis progression.

2 | MATERIALS AND METHODS

2.1 | Animals

Female *ApoE*$^{-/-}$ mice (#002052; Jackson Laboratory) were crossed with male *CD163*$^{-/-}$ mice (both on the C57BL/6 background), and the progeny bred back to *ApoE*$^{-/-}$ mice to obtain the double knockout (*ApoE*$^{-/-}$*CD163*$^{-/-}$) and their littermate control (*ApoE*$^{-/-}$*CD163*$^{-/-}$) mice. To study the effect of CD163 deletion on atherosclerotic lesions, 12-week-old *ApoE*$^{-/-}$*CD163*$^{-/-}$ (N = 10), and *ApoE*$^{-/-}$*CD163*$^{-/-}$ (N = 10) were fed on a hyperlipidemic diet (21.1% fat [0.15% cholesterol] +16.7% proteins) during 8 weeks. In addition, TWEAK-accelerated atherosclerosis was induced in 12-week-old *ApoE*$^{-/-}$*CD163*$^{-/-}$ (N = 10), and *ApoE*$^{-/-}$*CD163*$^{-/-}$ (N = 10) feeding a hyperlipidemic diet by murine TWEAK injection (5 μg/kg/three times per week; 1237-TW; R&D Systems) during the last 4 weeks. A fifth group of *ApoE*$^{-/-}$*CD163*$^{-/-}$ (N = 8) mice feeding a hyperlipidemic diet were injected with rCD163 (50 μg/kg/three times per week; 7435-CD; R&D Systems) and 2 hours later with TWEAK (5 μg/kg/three times per week) during the last 4 weeks.

All mice were maintained under barrier conditions. Water and diet were available ad libitum. At the end of the study, 16-hour fasted mice were anesthetized and euthanized by overdose of 100 mg/kg ketamine and 15 mg/kg xylazine and saline perfused. Blood samples were collected for biochemistry. Total serum cholesterol, HDL-c, and triglycerides were measured in our central laboratory (IIS-Fundación Jiménez Díaz). Serum Lactate Dehydrogenase (LDH) activity was measured with LDH colorimetric assay kit (ab102526; Abcam) following the manufacturer's instructions.

The housing and care of animals and all procedures carried out in this study were strictly in accordance with the Directive 2010/63/EU of the European Parliament and were approved by the Institutional Animal Care and Use Committee of IIS-Fundación Jiménez Díaz.

2.2 | Aortic root and brachiocephalic artery morphometric analysis

Brachiocephalic arteries (BCA) and hearts containing aortic roots were carefully dissected and frozen in OCT. Aortic roots were sectioned at 5 μm thickness beginning proximally at the first evidence of the aortic valves at their attachment site of aorta. Sections were stained with Oil red O/hematoxylin at 100 μm intervals from 0 to the end of the aortic valves. Maximal lesion area was calculated for each mouse by averaging the values for three sections. The individual maximal lesion areas were further averaged to determine the maximal lesion area for each group. Picrosirius red staining was performed for analysis of collagen content by measuring birefringence to plane-polarized light. Immunohistochemistry was carried out as previously described.[22]

To analyze the effect of CD163 deficiency on the progression of the atherosclerotic plaques in mice, we used the Stary method, which classified the atherosclerotic lesions based on their histological composition and structure[23]: grade I, early plaques containing only macrophages; grade II, lesions containing macrophages, VSMCs and a few cholesterol clefts; grade III, lesions containing macrophages, VSMCs and numerous cholesterol clefts; and grade IV, advanced plaques containing macrophages, VSMCs and a large lipid core.

Brachiocephalic arteries were serially sectioned in 5 μm thickness from the aortic root to the right subclavian artery. For morphometric analysis, sections of each brachiocephalic artery were stained with modified Russell-Movat pentachrome (Movat) at 90 μm intervals from 0 to 450 μm distal to the aortic root. The frequency of plaque instability features in each Movat-stained section was evaluated (5-6 slides per animal, 40 slides per group), including the following: necrotic core area, medial enlargement/erosion (defined as the replacement of the normal aorta by plaque components), and the presence of buried caps (signature of silent plaque rupture and confirmed by α-SMA staining). These parameters were recorded as binary outcome, and the frequency per lesion for each animal was determined with a 100% maximum possible.

2.3 | Immunohistochemical analysis

Immunohistochemical analysis was done as previously described.[24] Primary Abs were the monocyte/macrophage marker CD68 (Ab53444; Abcam), and the smooth muscle cell marker smooth muscle actin (Clone 1A4; Sigma). Goat anti-rat biotin (Amersham) was used as secondary antibodies. ABComplex/HRP was then added and sections were stained with AEC substrate-chromogen (DAKO), counterstained with hematoxylin, and mounted in Pertex (Medite). Incubation without primary Abs and/or irrelevant species- and isotype-matched immunoglobulins was used as a negative control for allimmunostainings. For colocalization studies anti-rat Alexa Fluor 568 was used as secondary Ab.

Computer-assisted morphometric analysis was performed with Image-Pro Plus software (version 1.0 for Windows). The threshold setting for area measurement was equal for all images. Samples from each animal were examined in a blinded manner. Results were expressed as % positive area vs total area (collagen, macrophages and α-actin) or $CD68^+$ cells vs total cells (BCA).

2.4 | Evans Blue permeability assays

ApoE$^{-/-}$*CD163*$^{+/+}$ and *ApoE*$^{-/-}$*CD163*$^{-/-}$ mice were intravenously injected with 20 mg/kg of 1% Evans blue dye (#E2129, Sigma-Aldrich), and perfused with saline after 30 minutes. Aorta, lungs, kidney, liver, and front and back legs were removed for later analysis. Tissues were weighed and Evans blue dye was extracted from different tissues by formamide at 56°C overnight. Evans blue was quantified by spectrophotometry at 595 nm. Results were expressed in ng of Evans Blue per mg of tissue.

2.5 | Cell culture

Aortic VSMCs were isolated from aorta of wild-type mice. Briefly, mice were anesthetized (100 mg/kg ketamine and 15 mg/kg xylazine), saline perfused, and aortas were isolated. Adhering fat and connective tissue were removed and vessels were sectioned in small rings and incubated in DMEM (Sigma) containing 1 mg/mL collagenase (type II, 290 U/mg), penicillin (100 U/mL), streptomycin (100 µg/mL), and glutamine (2 mmol/L) (Sigma) for 40 minutes at 37°C in 95% air/5% CO2. Then, the reaction was stopped with DMEM with 20% fetal bovine serum (FBS) and cells were seeded in plastic culture flasks (Costar) in DMEM with 20% FBS. Cells were harvested for passaging at 2- to 3-day intervals and used between the second and seventh passages. For experimental analysis, cells were made quiescent by 24-hour incubation in medium without FBS before stimulation with recombinant murine TWEAK (0.1 µg/mL; 1237-TW; R&D Systems) and preincubated or not with different concentrations of rCD163 (7435-CD; R&D Systems).

2.6 | Foam cell formation

Peritoneal macrophages were collected from *ApoE*-deficient or *ApoE/CD163* double-deficient mice by peritoneal lavage 4 days after intraperitoneal injection of 3% (wt/vol) thioglycolate. Cells were cultured 24 hours in RPMI supplemented with 10% FBS, L-glutamine, and antibiotics and then, stimulated for 48 hours in medium containing 2% FBS and 4 U/mL IL10 (11340103; Immunotools). After that, cells were incubated with 10 µg/mL Dil-ox-LDL for different time points. In some cases, cells were also treated with anti-CD36 antibody (2 µg/mL) (JC63.1; ab23680; Abcam) 1-hour prior Dil-ox-LDL incubation. Cells were fixed in 4% paraformaldehyde for 15 minutes and stained with DAPI. Percentage of foam cells were analyzed in 5-10 random different field per cell culture.

2.7 | Flow cytometry

For the uptake assays, peritoneal macrophages from *ApoE*-deficient or *ApoE/CD163* double deficient mice were washed once in PBS and incubated in RPMI media with IL-10 (4 U/mL) during 48 hours. After that, cells were incubated in fresh media containing Dil-ox-LDL (10 µg/mL; L34358; ThermoFisher Scientific) for 2 hours at 37°C. Then, cells were washed and resuspended in 0.5 mL of PBS and analyzed by flow cytometry.

For CD36 immunostaining, peritoneal macrophages from *ApoE*-deficient or *ApoE/CD163* double deficient mice were washed once in PBS and incubated in RPMI media with IL-10 (4 U/mL) during 48 hours. After that, cells were suspended in PBS containing 4% BSA, preincubated with Mouse BD Fc Block (553141; BD Pharmingen) for 10 minutes and costained for 18 hours at 4°C with anti-CD36 (Ab23680; Abcam). Alexa Fluor 488-conjugated goat anti-mouse (A11001; Life Technology) was used as secondary antibody. Cells were counted by flow cytometry using a BD FACS Canto II Flow Cytometer (BD Biosciences).

2.8 | PCR

Total RNA from VSMCs, peritoneal macrophages, or total aorta of mice was obtained by TRIzol method (Life Technologies) and quantified by absorbance at 260 nm in duplicate. Real-time PCR was performed on a TaqMan ABI 7700 Sequence Detection System using heat-activated TaqDNA polymerase (Amplitaq Gold). After an initial hold of 2 minutes at 50°C and 10 minutes at 95°C, the samples were cycled 40 times at 95°C for 15 seconds and 60°C for 60 seconds. A total of 18S rRNA served as housekeeping gene and was amplified in parallel with the genes of interest. The expression of target genes was normalized to housekeeping transcripts. The following PCR primers and TaqMan probes were purchased from Applied Biosystems and optimized according to the manufacturer's protocol: 18S (4310893E), mouse *CCL5* (Mm01302427), *CCL2* (Mm00441242), *MMP-2* (Mm00439498), *MMP-9* (Mm00442991), *CD163* (Mm00474091), and *ICAM-1* (00516023). All measurements were performed in triplicate. The amount of target mRNA in samples was estimated by the 2ΔCT relative quantification method. Values of each sample were obtained as multiples of their baseline values. Mouse mRNA levels for *Nos2*, *Arg1*, *SR-A*, *CD36*, *ABCG1*, and *ABCA1* were done by amplification of cDNA using SYBR Premix Ex TaqTM (Takara Biotechnology). The primer sequences are summarized in Table S1. The mRNA levels were normalized to the *GADPH* mRNA content.

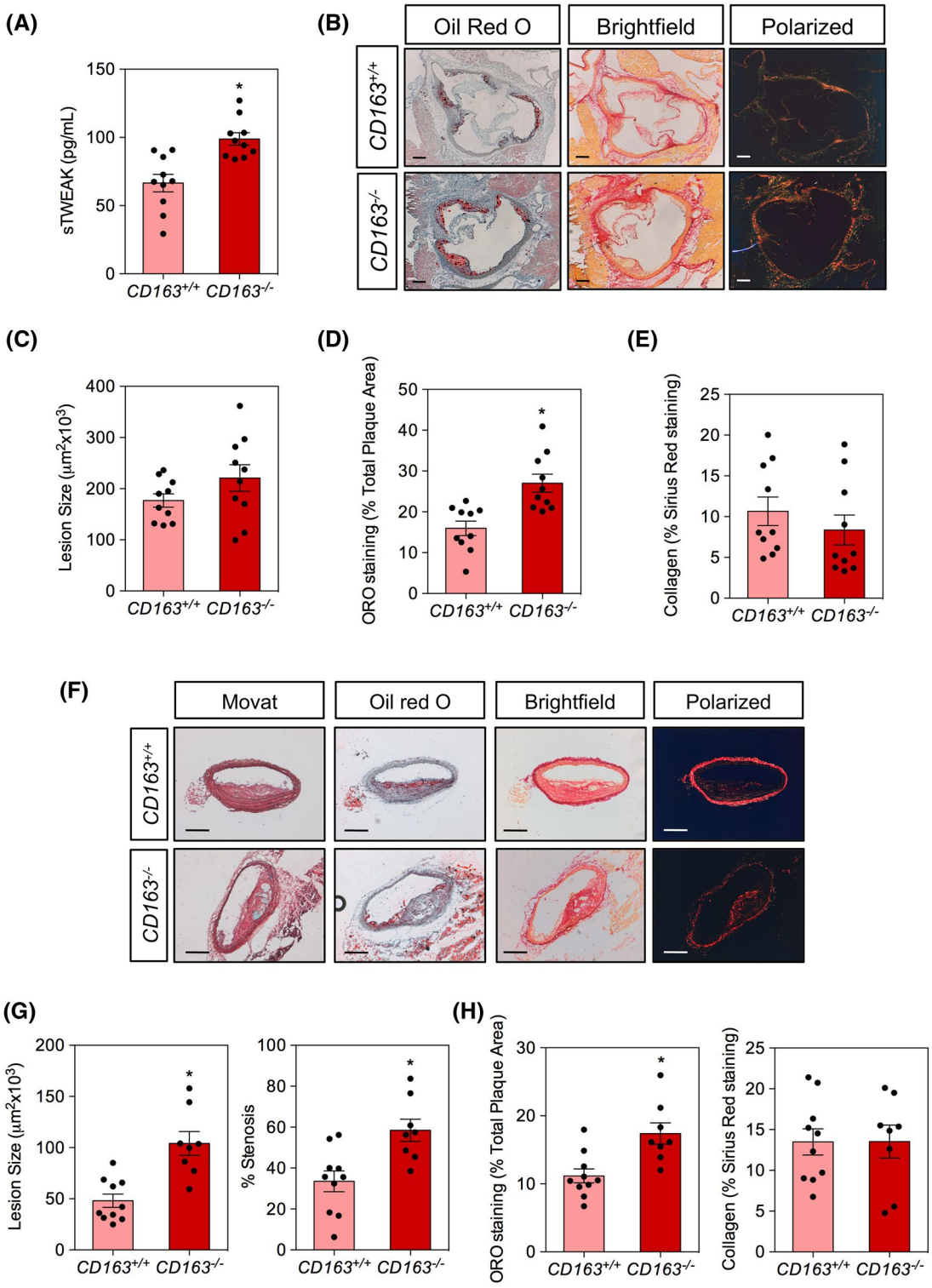

FIGURE 1 CD163 reduces atherosclerotic lesion size in *ApoE* knockout mice. A, sTWEAK serum concentrations in $ApoE^{-/-}CD163^{+/+}$ (n = 10) or $ApoE^{-/-}CD163^{-/-}$ (n = 10) mice at the end of the study. *$P < .001$, Student's *t* test. B, Representative Oil Red O/Hematoxylin and Sirius Red staining in $ApoE^{-/-}CD163^{+/+}$ and $ApoE^{-/-}CD163^{-/-}$ mice at the end of the study. Scale bars, 200 µm. C, Quantification of lesion area, (D) Oil Red O and (E) Sirius Red staining in the aortic root of $ApoE^{-/-}CD163^{+/+}$ and $ApoE^{-/-}CD163^{-/-}$ mice. Values shown are mean ± SEM of 10 animals per group. *$P < .01$, Student's *t* test. F, Representative photographs of Movat's pentachrome sections, Oil Red O/Hematoxylin and Sirius Red staining in the brachiocephalic artery from $ApoE^{-/-}CD163^{+/+}$ and $ApoE^{-/-}CD163^{-/-}$ mice. Scale bars, 200 µm. G, Quantification of lesion area, % stenosis, and (H) Oil Red O and Sirius Red staining in the brachiocephalic arteries of $ApoE^{-/-}CD163^{+/+}$ and $ApoE^{-/-}CD163^{-/-}$ mice. Values shown are mean ± SEM of 8-10 animals per group. *$P < .005$, Student's *t* test

2.9 | Migration assay

Migration of murine macrophages Raw 264.7 were measured in 8 μm pore transwell 24-well cell culture inserts (Costar). Cells were resuspended in DMEM with 0.2% BSA and seeded (70×10^4 per well) into the migration chamber. The lower wells of the chemotaxis chambers were filled with the supernatant of VSMCs in the different experimental conditions. After 4 hours of nonmigrating cells were removed from the upper part of the chamber and, the nuclei of migrated cells were fixated and stained with DAPI. The number of migrated cells was counted in

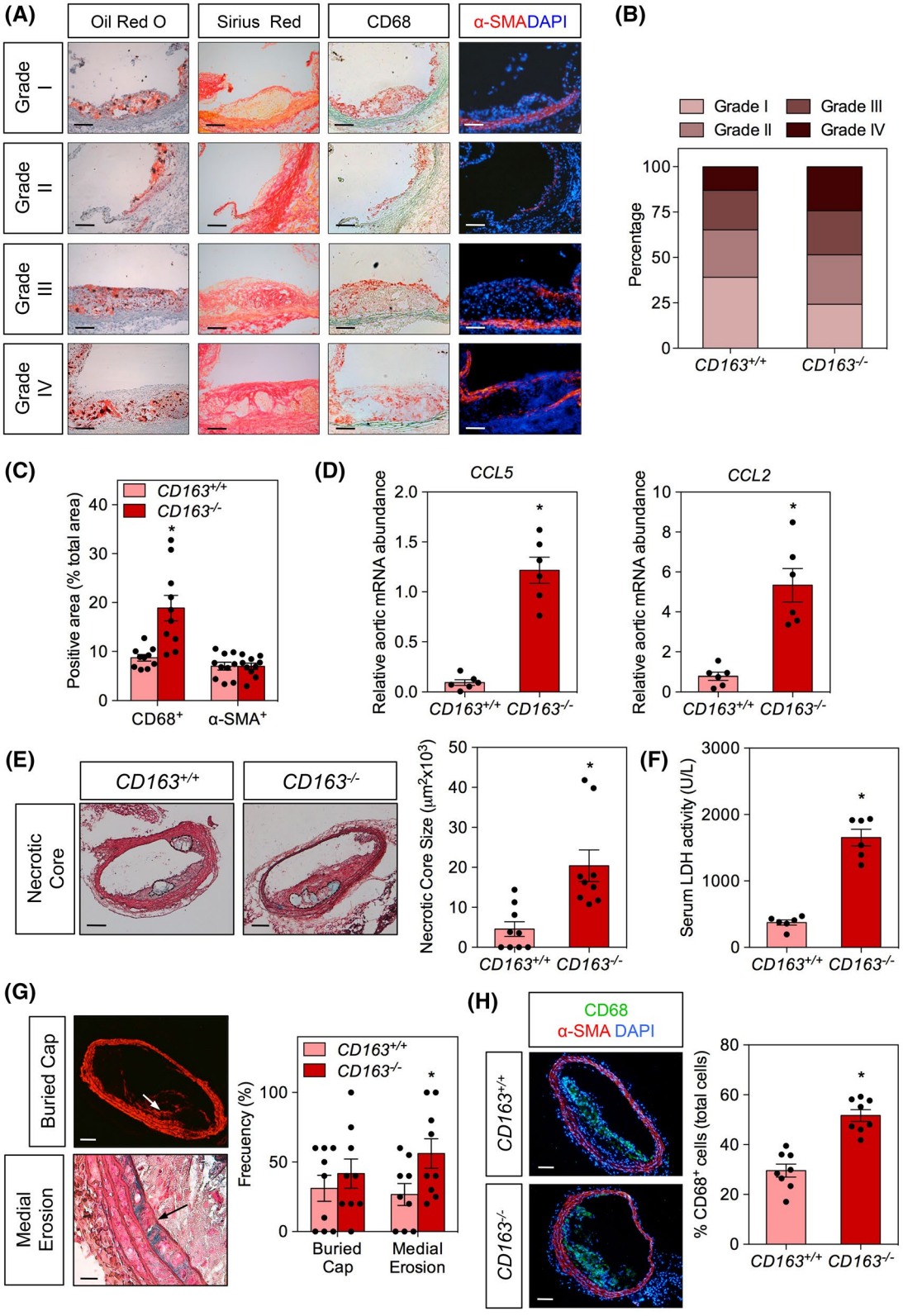

FIGURE 2 CD163 reduces plaque progression and diminishes features of plaque instability in *ApoE* knockout mice. A, Representative photographs of Oil Red O, Sirius red, α-SMA + DAPI, and CD68 stained sections classified according to the Stary method (grade I to IV). Scale bar, 100 μm. B, Percentage of each grade from Stary method between different groups. N = 25 plaques per group. C, Quantification of CD68 and α-SMA in aortic root from $ApoE^{-/-}CD163^{+/+}$ and $ApoE^{-/-}CD163^{-/-}$ mice. Values shown are mean ± SEM of 10 animals per group. *$P < .005$, Student's *t* test. D, Relative *CCL2* and *CCL5* mRNA expression levels normalized to 18S rRNA of aortas from $ApoE^{-/-}CD163^{+/+}$ or $ApoE^{-/-}CD163^{-/-}$ mice. Data represent the mean ± SEM of 6 animals per group; *$P < .001$, Student's *t* test. E, Representative images of BCA cross-sections stained with MOVAT from $ApoE^{-/-}CD163^{+/+}$ or $ApoE^{-/-}CD163^{-/-}$ mice. Dashed lines show the boundary of the developing necrotic area (NC). Quantification of the necrotic core area is shown in the below panel. Data represent the mean ± SEM of nine animals per group; *$P < .005$, Student's *t* test. Scale bar, 100 μm. F, LDH activity in serum from $ApoE^{-/-}CD163^{+/+}$ or $ApoE^{-/-}CD163^{-/-}$ mice. Data represent the mean ± SEM of six animals per group; *$P < .001$, Student's *t* test. G, Representative images of BCA cross sections showing the presence of buried cap (α-SMA staining) and medial erosion (MOVAT staining) in $ApoE^{-/-}CD163^{+/+}$ or $ApoE^{-/-}CD163^{-/-}$ mice. Below panel: Frequency of morphological markers of plaque instability in the below panel. Data represent the mean ± SEM of nine animals per group; *$P < .05$, Student's *t* test. Scale bar, 100 μm (25 μm for medial erosion). H, Representative images of BCA cross sections stained with α-SMA or CD68 from $ApoE^{-/-}CD163^{+/+}$ or $ApoE^{-/-}CD163^{-/-}$ mice. Quantification of CD68 positive cells is shown in the below panel. Data represent the mean ± SEM of eight animals per group; *$P < .001$, Student's *t* test. Scale bar, 100 μm

10-randomly selected fields by Nikon Eclipse E400 fluorescence microscope.

2.10 | Western blot

Cultured murine VSMCs from different experimental conditions were collected and lysated in lysis buffer containing 50 mM Tris-HCl pH 7.4, 150 mM NaCl, 2 mM EDTA, 2 mM EGTA, 0.2% Triton X-100, 0.3% NP-40, 0.2 mM PMSF, 0.2 mM Na_3VO_4, and 10 μL/mL of phosphatase inhibitor cocktail (P0044 Sigma) and pelleted. After normalizing for equal protein concentration, cell lysates were resuspended in SDS sample buffer before separation by SDS-PAGE as previously described (23). Following transfer of the proteins onto nitrocellulose membranes, membranes were probed using the following antibodies; NF-kB p65 (D14E12; Cell Signaling), phospho-NF-kB p65 (S536; Cell Signaling), and alpha-tubulin (T5168; Sigma).

2.11 | Cholesterol efflux

Peritoneal macrophages were isolated and labeled with [1α,2α(n)-3H]cholesterol (2 million of cells per well, 1 μCi per well) during 48 hours of incubation, as previously described.[25] Cells were washed and incubated with a serum-free medium (RPMI), which is supplemented with fatty acid-free BSA for 18 hours to allow equilibration of the radiolabeled cholesterol with the intracellular cholesterol pools. This experimental step was carried out under basal conditions of after adding liver X receptor (LXR) agonist T0901317 (4 μM) to induce the expression of ABCA1 and ABCG1 transporters. [3H]Cholesterol-labeled cells were then incubated for 4 hours at 37°C with a 5% dilution of murine apoB-depleted serum. Radioactivity was then measured in both medium and cells and the percentage of cholesterol efflux calculated.

2.12 | Statistical analysis

Data are expressed as mean ± the standard error of the mean (SEM). Kolmogorov-Smirnov test was used to assess normal distribution. Groups were compared with Student's *t* test or one-way ANOVA with Bonferroni's posttest. Significance was accepted at the level of $P < .05$. Statistical analysis was performed using GraphPad Prism 6.0 (GraphPad, San Diego, CA).

3 | RESULTS

3.1 | CD163 promotes beneficial plaque remodeling in an atherogenic environment

The main role of CD163 is to limit Hb toxicity within atherosclerotic plaques.[6] For that reason, we chose to investigate whether targeting CD163 in vivo would alter atherogenesis and plaque composition. To this end, 12-week-old mice lacking both *CD163* and *ApoE* ($ApoE^{-/-}CD163^{-/-}$) and their littermate $ApoE^{-/-}CD163^{+/+}$ single knockout mice were fed a hyperlipidemic diet for 8 weeks. No differences were observed in body weight or lipid concentrations between the different groups (Figure S1). Interestingly, $ApoE^{-/-}CD163^{-/-}$ mice presented increased sTWEAK plasma concentrations compared with $ApoE^{-/-}CD163^{+/+}$ mice (Figure 1A).

$ApoE^{-/-}CD163^{-/-}$ mice showed a non-significant 21% increase plaque size at the aortic root compared with $ApoE^{-/-}CD163^{+/+}$ mice (Figure 1B,C). However, when we analyzed other vascular territory (brachiocephalic arteries; BCA), a significant increment of 110% in plaque size and 58% in stenosis was observed in $ApoE^{-/-}CD163^{-/-}$ mice compared with their littermate mice (Figure 1F,G).

Whereas collagen fibers stabilize atherosclerotic plaques, lipid depositions make plaques more prone to rupture.[26]

ApoE$^{-/-}$*CD163*$^{-/-}$ mice exhibited increased Oil Red O (ORO) content in atherosclerotic plaques present in both aortic root (Figure 1B,D) and BCA (Figure 1F,H) compared with *ApoE*$^{-/-}$*CD163*$^{+/+}$ mice. Collagen content was similar in atherosclerotic lesions present in aortic root (Figure 1B,E) or BCA (Figure 1F,H) of both genotypes.

To analyze the effect of CD163 deficiency in the progression of the atherosclerotic plaques in mice, we used the Stary method[23] (Figure 2A). Approximately 40% plaques in *ApoE*$^{-/-}$*CD163*$^{+/+}$ mice were early lesions (grade I) while only ≈13% plaques were advanced plaques (grade IV) (Figure 2B). In contrast, the percentage of advanced plaques

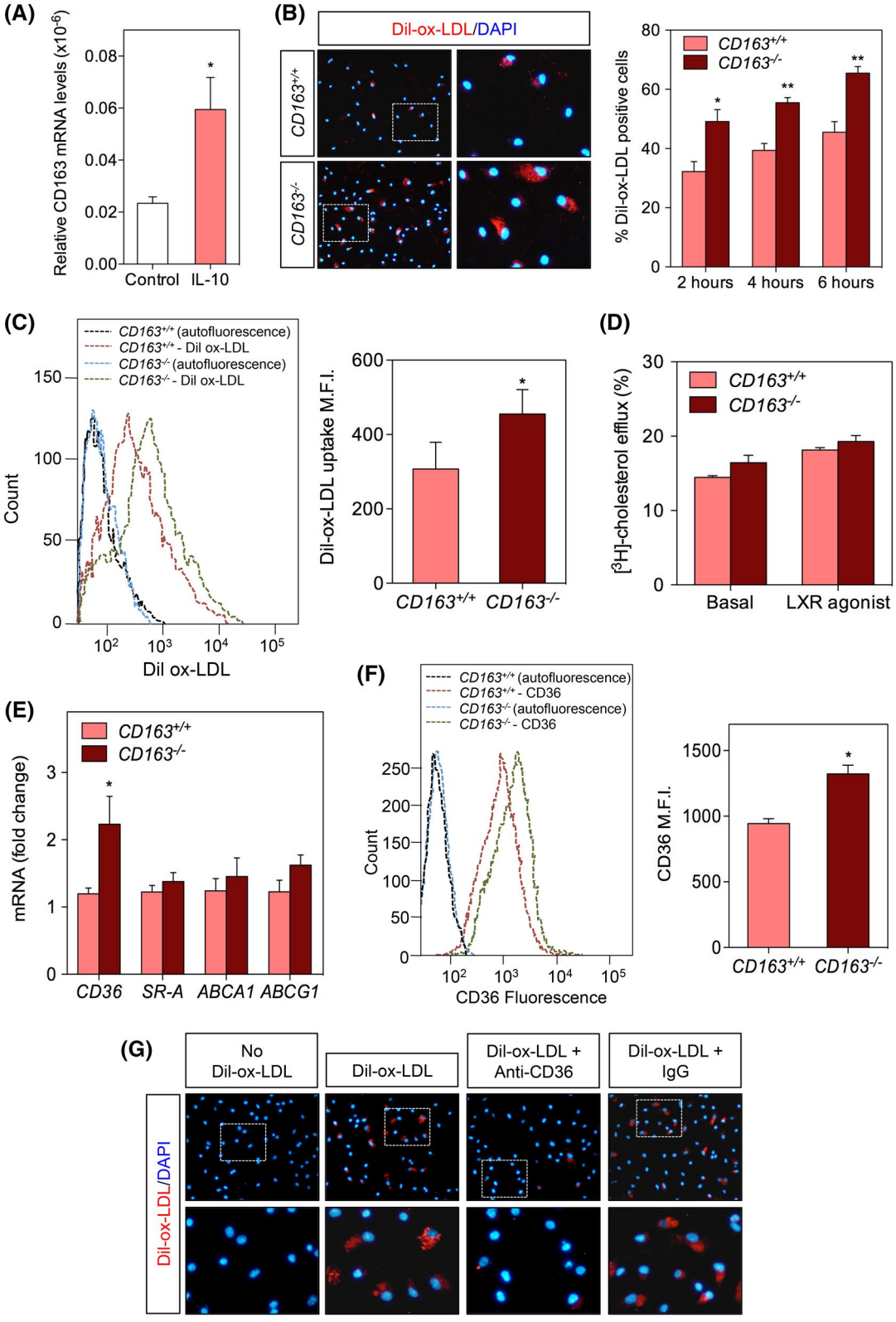

FIGURE 3 Absence of CD163 promotes foam cell formation. A, Relative *CD163* mRNA expression levels normalized to 18S rRNA of peritoneal macrophages from $ApoE^{-/-}CD163^{+/+}$ mice treated with IL-10 (4 ng/mL) during 48 hours. Data represent the mean ± SEM of three independent experiments; $*P < .05$; Student's *t* test. B, Representative images of $ApoE^{-/-}CD163^{+/+}$ or $ApoE^{-/-}CD163^{-/-}$ peritoneal macrophages incubated with or without Dil-ox-LDL (10 μg/mL) for 4 hours. Quantification of Dil-ox-LDL positive cells incubated with or without Dil-ox-LDL for 2-6 hours in the right panel. Data represent the mean ± SEM of four independent experiments; $*P < .05$ and $**P < .005$; Student's *t* test. Scale bars, 50 μm (low magnification); 20 μm (High magnification). C, Flow cytometry analysis of Dil-ox-LDL uptake in peritoneal macrophages of $ApoE^{-/-}CD163^{+/+}$ or $ApoE^{-/-}CD163^{-/-}$ incubated with Dil-ox-LDL (10 μg/mL) for 2 hours. The results are expressed in terms of geometric mean fluorescence intensity (MFI) after subtracting the autofluorescence of cells incubated in absence of Dil-ox-LDL. Data represent the mean ± SEM of four independent experiments. $*P < .05$; Student's *t* test. D, Cholesterol efflux to ApoB-depleted plasma in peritoneal macrophages from $ApoE^{-/-}CD163^{+/+}$ or $ApoE^{-/-}CD163^{-/-}$ stimulated with or without LXR agonist. Data represent mean ± SEM of duplicate samples (n = 3 per group). E, Relative *CD36, SR-A, ABCA1, and ABCG1* mRNA expression levels normalized to 18S rRNA of peritoneal macrophages from $ApoE^{-/-}CD163^{+/+}$ mice treated with IL-10 (4 ng/mL) during 48 hours. Data represent the mean ± SEM of five independent experiments; $*P < .05$; Student's *t* test. F, Flow cytometry analysis of CD36 expression in peritoneal macrophages of $ApoE^{-/-}CD163^{+/+}$ or $ApoE^{-/-}CD163^{-/-}$ incubated with IL-10 (4 ng/mL) during 48 hours. The results are expressed in terms of geometric mean fluorescence intensity (MFI) after subtracting the autofluorescence of cells incubated in absence of CD36 antibody. Data represent the mean ± SEM of four independent experiments. $*P < .05$; Student's *t* test. G, Representative images of $ApoE^{-/-}CD163^{-/-}$ peritoneal macrophages incubated with or without Dil-ox-LDL (10 μg/mL) for 4 hours. Anti-CD36 was preincubated 1 hour before Dil-ox-LDL treatment. IgG was used as control

was ≈25% in $ApoE^{-/-}CD163^{-/-}$ mice while ≈23% plaques were early lesions (Figure 2B). To further confirm that CD163 is negatively associated to plaque progression, we analyzed the BCA for other features that both associate with and contribute to diminish plaque stability such as necrotic core size, and the presence of medial erosion and buried caps.[27] These features are more evident in BCA than in the aortic root. $ApoE^{-/-}CD163^{-/-}$ mice exhibited an increased necrotic core size (Figure 2E). Accordingly, LDH activity, a marker of tissue damage, was increased in serum from $ApoE^{-/-}CD163^{-/-}$ mice compared to $ApoE^{-/-}CD163^{+/+}$ mice (Figure 2F). A higher frequency of medial erosion was also observed in $ApoE^{-/-}CD163^{-/-}$ mice compared to $ApoE^{-/-}CD163^{+/+}$ mice (Figure 2G).

Inflammation has a great impact on the vulnerability of atherosclerotic plaques.[28] *CD163*-deficient atherosclerotic lesions showed a 96% increase in the CD68 positive area in the aortic sinus (Figure 2C) and 74% increase in CD68 positive cells in BCA cross-section analysis (Figure 2H). No changes were observed in the levels of smooth muscle actin (Figure 2C,G, Figure S2). Monocytes infiltrate atherosclerotic lesions in response to pro-inflammatory cytokines such as CCL2 and CCL5. *CD163*-deficient aortas showed an increase in *CCL2* and *CCL5* mRNA expression (Figure 2D), indicating that the presence of CD163 modulates monocyte infiltration. No changes in vascular permeability were observed between $ApoE^{-/-}CD163^{+/+}$ and $ApoE^{-/-}CD163^{-/-}$ mice (Figure S3).

A continuum of pro- and anti-inflammatory macrophages, with extreme polarized phenotypes, can be found in atherosclerotic lesions.[29] Since CD163 is considered a marker of M2-type macrophages, we tested whether CD163 deficiency can influence macrophage polarization. No changes were observed in the mRNA expression of *Nos2*-M1 or *Arg1*-M2 genetic markers in the aorta from $ApoE^{-/-}CD163^{+/+}$ or $ApoE^{-/-}CD163^{-/-}$ mice (Figure S4).

Collectively, these results demonstrate that CD163 deficiency increases the macrophages infiltration and plaque progression in hyperlipidemic mice.

3.2 | *CD163* deficiency increases foam cell formation by CD36 upregulation

Macrophage foam cell formation as a result of the excess of lipid deposition is an important step in atherosclerotic plaque development.[30] Since we have observed that CD163-deficient mice showed atheroma plaques with higher number of macrophages and higher intracellular lipids content, we analyzed the importance of CD163 to control macrophage functions. To this end, peritoneal macrophages from both $ApoE^{-/-}CD163^{+/+}$ and $ApoE^{-/-}CD163^{-/-}$ mice were incubated with IL-10 (4 ng/mL; 48 hours), the best interleukin to produce CD163-expressing macrophages[31] (Figure 3A).

After that, macrophages were incubated with fluorescently labeled Dil-ox-LDL (10 μg/mL; 2-6 hours) and assessed lipid content by fluorescence incorporation. We found that a higher percentage of $ApoE^{-/-}CD163^{-/-}$ macrophages stimulated with Dil-ox-LDL accumulate more lipids than $ApoE^{-/-}CD163^{+/+}$ macrophages (Figure 3B), suggesting that CD163 deficiency increases foam cell formation. The increased lipid accumulation in $ApoE^{-/-}CD163^{-/-}$ macrophages could be an outcome of either increased uptake of modified LDL or decreased cholesterol efflux. To analyze these possibilities, we performed uptake assays by incubating peritoneal macrophages isolated from $ApoE^{-/-}CD163^{+/+}$ and $ApoE^{-/-}CD163^{-/-}$ mice with Dil-ox-LDL and quantified the uptake by flow cytometry. There was more uptake of Dil-ox-LDL in *CD163*-deficient than in *CD163*-expressing macrophages (Figure 3C). In addition, no differences were observed in cholesterol efflux to ApoB-depleted serum in macrophages under basal conditions or stimulated with LXR agonist

T0901217 (Figure 3D). In peritoneal macrophages, we analyzed the expression of SR-A and CD36 scavenger receptors, and ATP-binding cassette transporters ABCG1 and ABCA1, the main transporters responsible for cholesterol efflux in macrophages. We observed an increase in *CD36* mRNA and protein expression in $ApoE^{-/-}CD163^{-/-}$ macrophages compared to $ApoE^{-/-}CD163^{+/+}$ macrophages (Figure 3E,F), while *SR-A*, *ABCG1*, and *ABCA1* mRNA expression was similar between both types of macrophages (Figure 3E). Preincubation with anti-CD36 inhibited Dil-ox-LDL uptake by $ApoE^{-/-}CD163^{-/-}$ macrophages (Figure 3G). Collectively, these results demonstrate that loss of CD163 increase the

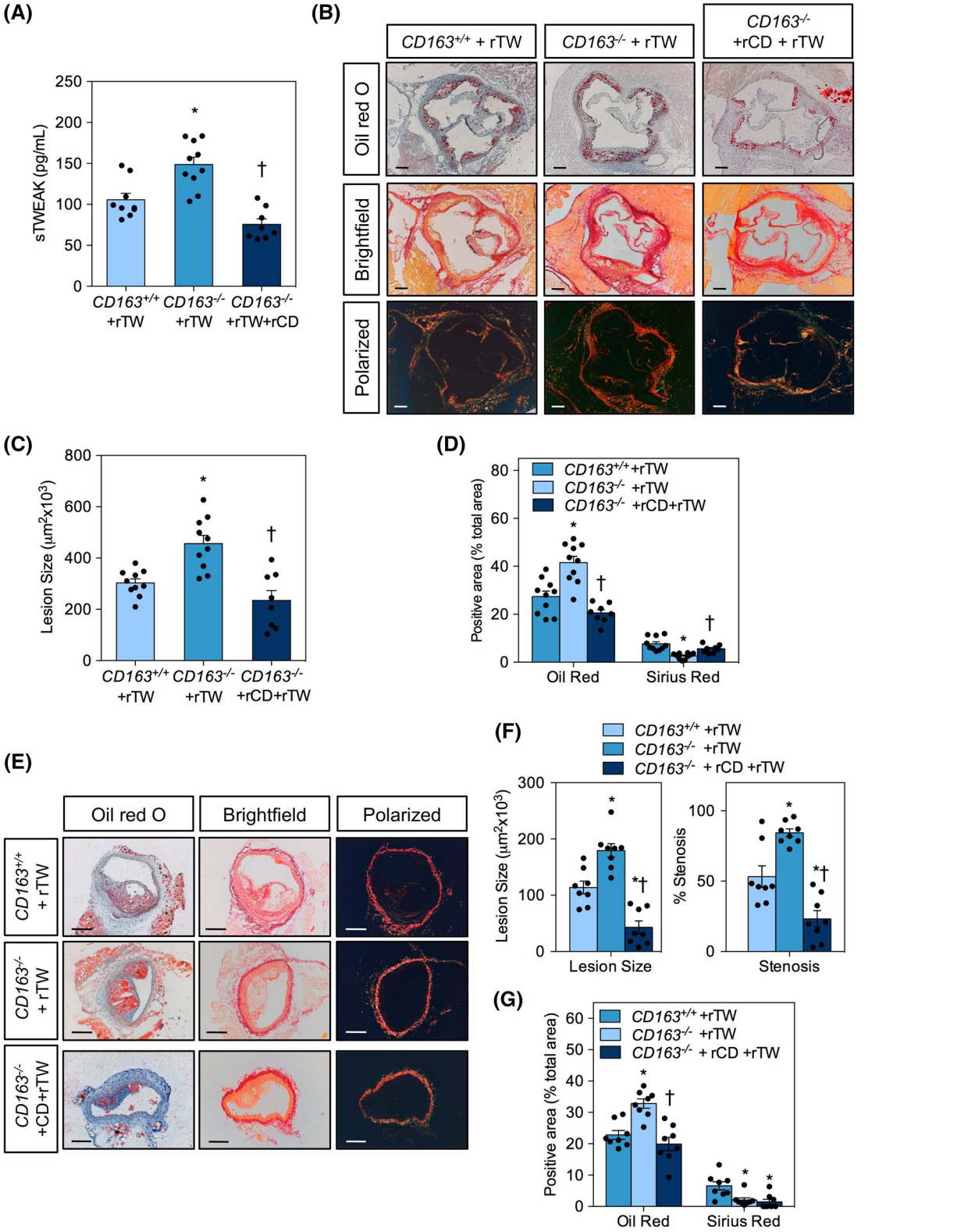

FIGURE 4 TWEAK increases atherosclerotic lesion size in CD163 deficient mice. A, sTWEAK serum concentrations in *ApoE*$^{-/-}$*CD163*$^{+/+}$ (n = 10) or *ApoE*$^{-/-}$*CD163*$^{-/-}$ (n = 10) mice treated with recombinant TWEAK (rTWEAK; 5 μg/kg/three times per week) and *ApoE*$^{-/-}$*CD163*$^{-/-}$ (N = 8) treated with recombinant CD163 (rCD; 50 μg/kg/three times per week) 2 hours before rTWEAK administration. *$P < .01$ vs *ApoE*$^{-/-}$*CD163*$^{+/+}$ + rTW; $^{\dagger}P < .001$ vs *ApoE*$^{-/-}$*CD163*$^{-/-}$ + rTW; One-way ANOVA with Bonferroni's posttest. B, Representative Oil Red O/Hematoxylin and Sirius Red staining in *ApoE*$^{-/-}$*CD163*$^{+/+}$ and *ApoE*$^{-/-}$*CD163*$^{-/-}$ mice with the different treatments at the end of the study. Scale bars, 100 μm. C, Quantification of lesion area, (D) Oil Red O and Sirius Red staining in the aortic root of *ApoE*$^{-/-}$*CD163*$^{+/+}$ and *ApoE*$^{-/-}$*CD163*$^{-/-}$ mice treated with rTW alone or rTW and rCD. Values shown are mean ± SEM of 8-10 animals per group. *$P < .01$ *vs* *ApoE*$^{-/-}$*CD163*$^{+/+}$ + rTW. $^{\dagger}P < .01$ vs *ApoE*$^{-/-}$*CD163*$^{-/-}$ + rTW; One-way ANOVA with Bonferroni's posttest. E, Representative photographs of Movat's pentachrome sections, Oil Red O/Hematoxylin and Sirius Red staining in the brachiocephalic artery from *ApoE*$^{-/-}$*CD163*$^{+/+}$ and *ApoE*$^{-/-}$*CD163*$^{-/-}$ mice treated with rTW alone or rTW and rCD. Scale bars, 200 μm. F, Quantification of lesion area and % stenosis in the BCA of *ApoE*$^{-/-}$*CD163*$^{+/+}$ and *ApoE*$^{-/-}$*CD163*$^{-/-}$ mice treated with rTW alone or rTW and rCD. Values shown are mean ± SEM of eight animals per group. *$P < .01$ *vs* *ApoE*$^{-/-}$*CD163*$^{+/+}$; $^{\dagger}P < .001$ vs *ApoE*$^{-/-}$*CD163*$^{-/-}$ + rTW, One-way ANOVA with Bonferroni's posttest. G, Oil Red O and Sirius Red staining in the BCA of *ApoE*$^{-/-}$*CD163*$^{+/+}$ and *ApoE*$^{-/-}$*CD163*$^{-/-}$ mice treated with rTW alone or rTW and rCD. Values shown are mean ± SEM of 8 animals per group. *$P < .01$ *vs* *ApoE*$^{-/-}$*CD163*$^{+/+}$ + rTW; One-way ANOVA with Bonferroni's posttest

CD36 expression and modified ox-LDL uptake promoting macrophage foam cell formation.

3.3 | TWEAK aggravates atherosclerosis progression in *CD163*-deficient mice

Next, we investigated the potential role of CD163 as a scavenger receptor in TWEAK-induced atherosclerosis.[20] First, we administered recombinant murine TWEAK (rTW; 5 μg/kg/three times per week) into either *ApoE*$^{-/-}$*CD163*$^{+/+}$ or *ApoE*$^{-/-}$*CD163*$^{-/-}$ mice and examined atherosclerotic lesions 4 weeks later. No differences were observed in body weight or lipid concentrations between the different groups (Figure S1). *ApoE*$^{-/-}$*CD163*$^{-/-}$ mice presented increased sTWEAK plasma concentrations compared with *ApoE*$^{-/-}$*CD163*$^{+/+}$ mice after rTW administration (Figure 4A). *ApoE*$^{-/-}$*CD163*$^{-/-}$ mice treated with rTW showed a significant 51% increase plaque size at the aortic root (Figure 4B,C) and in plaque size (62%) and in stenosis (58%) at the BCA (Figure 4E-F) compared with their littermate mice. *ApoE*$^{-/-}$*CD163*$^{-/-}$ mice treated with rTW also exhibited increased ORO and reduced collagen content in atherosclerotic plaques present in both the aortic root (Figure 4B,D) and BCA (Figure 4E-G) compared with infused *ApoE*$^{-/-}$*CD163*$^{+/+}$ mice.

When plaque progression was analyzed, ≈17% plaques in *ApoE*$^{-/-}$*CD163*$^{+/+}$ mice treated with rTW were early lesions (grade I) while ≈33% plaques were advanced plaques (grade IV). In contrast, the percentage of advanced lesion was 46% in *ApoE*$^{-/-}$*CD163*$^{-/-}$ mice treated with rTW while only ≈8% plaques were early lesions (Figure 5B). *ApoE*$^{-/-}$*CD163*$^{-/-}$ mice treated with rTW showed a 54% increase in macrophage content in the aortic root (Figure 5A) and 51% increase in CD68^{+} cells in BCA (Figure 5G), and aortic CCL2 and CCL5 mRNA expression (Figure 5C), compared with *ApoE*$^{-/-}$*CD163*$^{+/+}$ mice. No changes were observed in the mRNA expression of *Nos2*-M1 or *Arg1*-M2 genetic markers in the aorta from *ApoE*$^{-/-}$*CD163*$^{+/+}$ or *ApoE*$^{-/-}$*CD163*$^{-/-}$ mice treated with rTW (Figure S4). In addition, no changes were observed in the levels of α-SMA (Figure 5A,F, Figure S2). Finally, BCA from *ApoE*$^{-/-}$*CD163*$^{-/-}$ mice treated with rTW exhibited an increased necrotic core size (Figure 5D), serum LDH activity (Figure 5E), and a higher frequency of buried caps and medial erosion (Figure 5F) than atherosclerotic plaques from *ApoE*$^{-/-}$*CD163*$^{+/+}$ mice.

In a second approach, we analyzed whether the systemic soluble CD163 can abolish the proatherogenic effects of TWEAK. For that purpose, a third group of animals were injected with recombinant murine soluble CD163 (rCD; 50 μg/kg/three times per week) 2 hours before rTW administration. No differences were observed in body weight or lipid concentrations after rCD administration (Figure S1). *ApoE*$^{-/-}$*CD163*$^{-/-}$ mice injected with both rCD and rTW presented decreased sTWEAK plasma concentrations compared with *ApoE*$^{-/-}$*CD163*$^{-/-}$ mice treated with rTW alone (Figure 4A). In *ApoE*$^{-/-}$*CD163*$^{-/-}$ mice, rCD163 administration diminished 50% and 76% the plaque size in both, aortic root and BCA, respectively (Figure 4B,C,E,F). In addition, rCD decreased ORO content (Figure 4D,G) and showed a 58% reduction in macrophage content in the aortic root (Figure 5A) and 64% reduction in CD68^{+} cells in BCA (Figure 5G), as well as aortic CCL2 and CCL5 mRNA expression (Figure 5C), compared with *ApoE*$^{-/-}$*CD163*$^{-/-}$ mice treated with rTW alone. No changes were observed in the levels of α-SMA (Figure 5A,F, Figure S2). When plaque progression was analyzed, in contrast to the effect observed in rTW-injected *ApoE*$^{-/-}$*CD163*$^{-/-}$ mice, in rCD and rTW-injected *ApoE*$^{-/-}$*CD163*$^{-/-}$ mice, ≈40% plaques were early lesions (grade I) while ≈20% plaques were advanced plaques (grade IV). In addition, BCA from rCD-injected *ApoE*$^{-/-}$*CD163*$^{-/-}$ mice exhibit a decreased necrotic core size (Figure 5D), less serum LDH activity (Figure 5E) and a lesser frequency of buried caps and medial erosion (Figure 5F) than atherosclerotic plaques from rTW-treated *ApoE*$^{-/-}$*CD163*$^{-/-}$ mice.

Overall, these in vivo experiments could indicate that deficiency of CD163 increases TWEAK availability enhancing its proatherogenic effects.

3.4 | CD163 inhibits TWEAK-induced inflammatory responses in VSMCs and macrophage migration

To determine how CD163 regulates the effect of TWEAK-induced inflammation during atherosclerotic plaque development, VSMCs and macrophages were studied in vitro. TWEAK regulates several pro-inflammatory molecules in VSMCs through nuclear factor kappa B activation.[32] We have shown herein that addition of rCD163 to TWEAK-stimulated cultured VSMCs can inhibit the biological effects of TWEAK on NF-kB signaling, (Figure 6A). In addition,

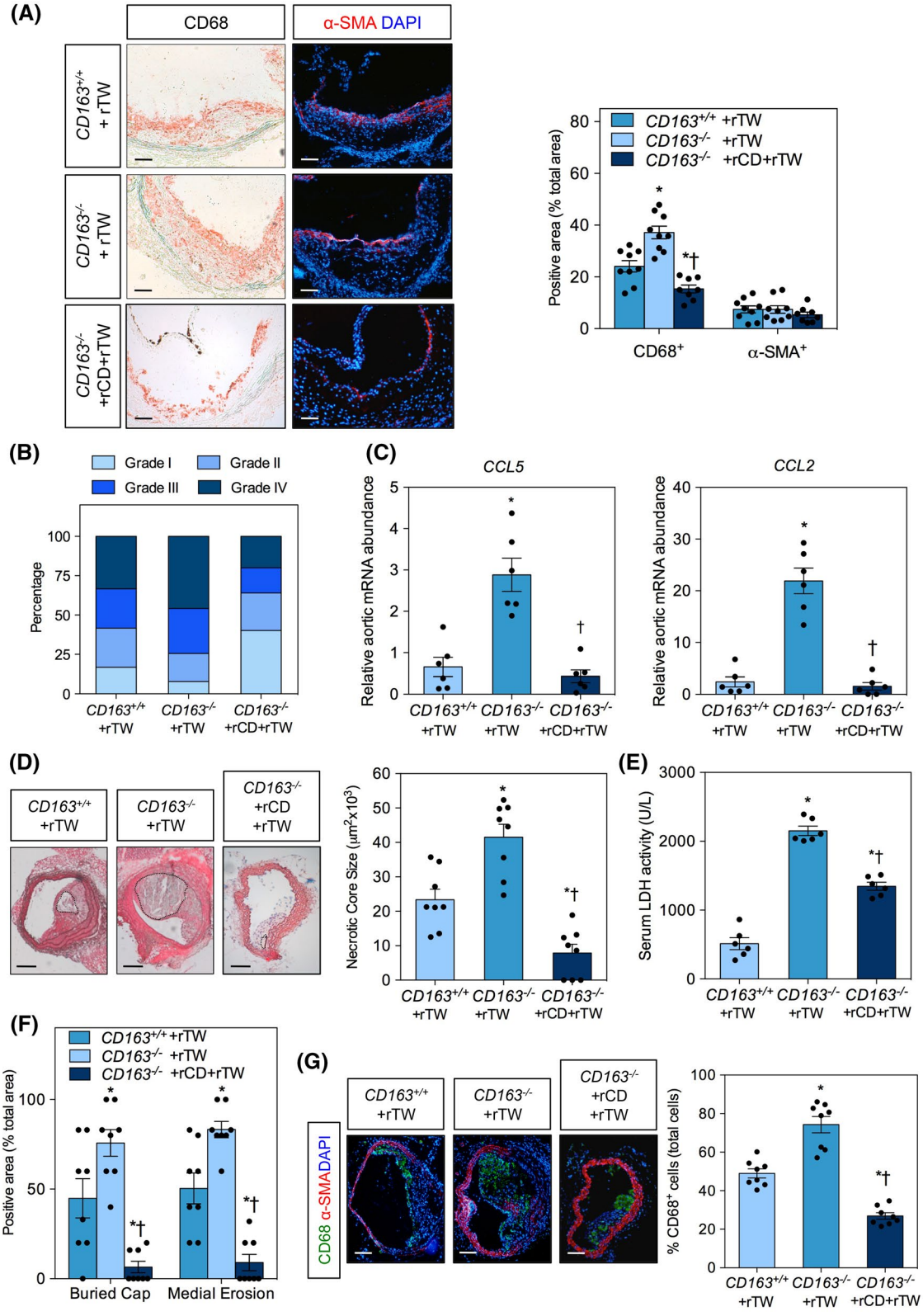

FIGURE 5 TWEAK enhances plaque instability in CD163 deficient mice. A, Representative photographs of α-SMA + DAPI and CD68 stained sections. Quantification of CD68 and α-SMA in aortic root from *ApoE*$^{-/-}$*CD163*$^{+/+}$ and *ApoE*$^{-/-}$*CD163*$^{-/-}$ mice treated with rTW alone or rTW plus rCD in the right panel. Values shown are mean ± SEM of 8-9 animals per group. **P* < .05 vs *ApoE*$^{-/-}$*CD163*$^{+/+}$; †*P* < .001 vs *ApoE*$^{-/-}$*CD163*$^{-/-}$ + rTW; One-way ANOVA with Bonferroni's posttest. Scale bar, 100 μm. B, Percentage of each grade from Stary method between different groups. N = 20-25 plaques per group. C, Relative *CCL2* and *CCL5* mRNA expression levels normalized to 18S rRNA of aortas from *ApoE*$^{-/-}$*CD163*$^{+/+}$ or *ApoE*$^{-/-}$*CD163*$^{-/-}$ mice treated with rTW alone or rTW plus rCD. Data represent the mean ± SEM of six animals per group; **P* < .001 vs *ApoE*$^{-/-}$*CD163*$^{+/+}$ + rTW. †*P* < .001 vs *ApoE*$^{-/-}$*CD163*$^{-/-}$ + rTW; One-way ANOVA with Bonferroni's posttest. D, Representative images of BCA cross sections stained with MOVAT from *ApoE*$^{-/-}$*CD163*$^{+/+}$ or *ApoE*$^{-/-}$*CD163*$^{-/-}$ mice treated with rTW alone or rTW plus rCD. Dashed lines show the boundary of the developing necrotic area (NC). Quantification of the necrotic core area is shown in the below panel. Data represent the mean ± SEM of eight animals per group; **P* < .05 vs *ApoE*$^{-/-}$*CD163*$^{+/+}$; †*P* < .001 vs *ApoE*$^{-/-}$*CD163*$^{-/-}$ + rTW; One-way ANOVA with Bonferroni's posttest. Scale bar, 100 μm. E, LDH activity in serum from *ApoE*$^{-/-}$*CD163*$^{+/+}$ and *ApoE*$^{-/-}$*CD163*$^{-/-}$ mice treated with rTW alone or rTW and rCD. Data represent the mean ± SEM of six animals per group; **P* < .001, *vs ApoE*$^{-/-}$*CD163*$^{+/+}$ + rTW. †*P* < .001 vs *ApoE*$^{-/-}$*CD163*$^{-/-}$ + rTW. One-way ANOVA with Bonferroni's posttest. F, Frequency of morphological markers of plaque instability in *ApoE*$^{-/-}$*CD163*$^{+/+}$ or *ApoE*$^{-/-}$*CD163*$^{-/-}$ mice treated with rTW alone or rTW plus rCD. Data represent the mean ± SEM of eight animals per group; **P* < .05 vs *ApoE*$^{-/-}$*CD163*$^{+/+}$ + rTW. †*P* < .001 vs *ApoE*$^{-/-}$*CD163*$^{-/-}$ + rTW; One-way ANOVA with Bonferroni's posttest. G, Representative images of BCA cross sections stained with α-SMA or CD68 from *ApoE*$^{-/-}$*CD163*$^{+/+}$ or *ApoE*$^{-/-}$*CD163*$^{-/-}$ mice treated with rTW alone or rTW plus rCD. Quantification CD68 positive cells is shown in the below panel. Data represent the mean ± SEM of eight animals per group; **P* < .05 vs *ApoE*$^{-/-}$*CD163*$^{+/+}$ + rTW; †*P* < .001 vs *ApoE*$^{-/-}$*CD163*$^{-/-}$ + rTW; One-way ANOVA with Bonferroni's posttest. Scale bar, 100 μm

rTW increased *CCL2*, *CCL5*, *ICAM-1*, and *MMP-9* mRNA expression and CCL2 and CCL5 secretion in VSMCs, which was abolished when increased concentrations of rCD163 were present in the culture media (Figure 6B,C).

The inflammatory environment mediated by VSMCs during atheroma plaques formation is also responsible for the recruitment of the immune cells, especially monocyte/macrophages. As we have observed that the percentage of macrophages in plaques also depends on the presence of CD163, we analyzed the macrophages migratory capacity upon different inflammatory scenarios. VSMCs were stimulated with rTW in the absence or presence of increased amount of rCD for 24 hours. After that, the supernatants were collected and incubated with RAW 264.7 cell for 4 hours and cell migration was tested using an in vitro transwell migration assay. As expected, supernatant of rTW-stimulated VSMCs significantly increased macrophage migration compared with medium alone (Figure 6D). In addition, RAW migration was inhibited in a dose-dependent manner upon incubation with supernatant obtained from VSMCs treated with both, rTW and rCD (Figure 6D). Overall, these data indicate that CD163 is able to block the pro-inflammatory response induced by TWEAK in VSMCs, decreasing macrophages recruitment.

4 | DISCUSSION

Different populations of macrophages reside in human atherosclerotic plaques and microenvironment within plaques plays a pivotal role in the differentiation program of macrophages.[33] M2-type macrophages promote the resolution of inflammation and tissue repair. In fact, the conversion of Ly6C^{high} monocytes in M2-type macrophages drives atherosclerosis regression in mice.[34] These macrophages are characterized by expressing high levels of CD163,[5,35] a protein expressed in human coronary, aortic and femoral lesions.[6,10,36] A principal function of CD163 in atherosclerotic plaques might be to remove Hp-Hb complexes in intralesional hemorrhage. In fact, hemoglobin uptake by CD163-expressing macrophages leads to a distinct macrophage phenotype termed M(Hb) or Mhem.[37] M(Hb) macrophages are abundant in areas of neoangiogenesis and hemorrhage characterized by reduced cytokine production and a lack of lipid retention.[11,37,38] For those reasons, M(Hb) macrophages have been considered atheroprotective. However, it has been recently reported that M(Hb) macrophages promote angiogenesis and vascular permeability accompanied by inflammation in atherosclerosis.[11] Although Hb is a key inductor of CD163 expression, stimulation of macrophages with other molecules such as pro- and anti-inflammatory cytokines can also induce the polarization to M2-type macrophages and modulates CD163 expression in absence of Hb. In fact, INF-γ or TNF-α decrease and IL-6 or IL-10 increase CD163 expression in macrophages.[31] It is important to note that contrary to human haptoglobin (Hp), mouse Hp does not promote high-affinity binding to CD163. Nevertheless, mouse hemoglobin (Hb) has a higher CD163 affinity than human Hb. The overall clearance of Hb is slower in CD163-deficient mice, and its accumulated in the liver. However, the ratio of mHb/mHpHb in serum is similar in *CD163*$^{+/+}$ and *CD163*$^{-/-}$ mice.[39]

In vitro experiments have demonstrated that CD163-expressing macrophages can also bind and internalize TWEAK.[12,40] Now, we used *CD163*-deficient mice to demonstrate an important role of CD163 in the setting of atherosclerotic plaque development and progression. We have observed that the loss of CD163 increases soluble TWEAK concentrations in *ApoE*-deficient mice. According to the pro-inflammatory and proatherogenic

actions of TWEAK,[20-22] *CD163*-deficient mice showed an increase of plaque size in BCA. Clinically, lesion composition rather than size or degree of stenosis of the lesion determines the likehood of plaque rupture and subsequent thrombotic complications.[41] *CD163*-deficient mice showed a larger necrotic core and an increase in lipid content, macrophage infiltration and pro-inflammatory cytokines expression in atherosclerotic lesions. Opposite to our results, it has been recently reported that *ApoE*-deficient mice showed an increase in BCA plaque area compared with

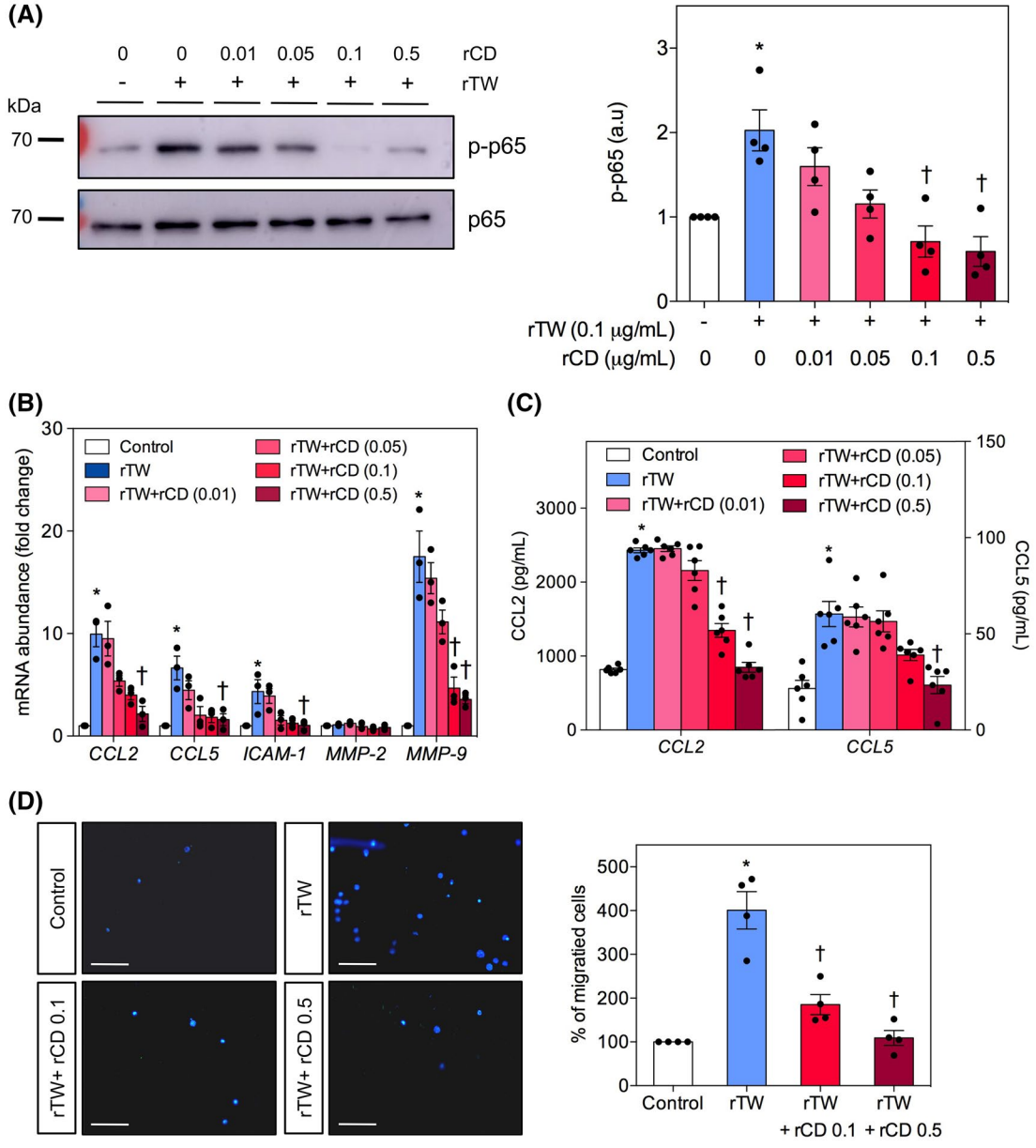

FIGURE 6 CD163 prevents pro-inflammatory actions induced by TWEAK. A, Representative western blot analysis of p-p65 and p65 in VSMCs treated with 0% FBS (control), rTW (100 ng/mL) or rTW plus rCD (0.01-0.5 µg/mL). Right panel show the quantification of band densitometry values of p-p65 protein levels expressed in arbitrary units after correction for p65 (loading control). *$P < .01$ vs Control; †$P < .01$ vs rTW; Student's *t* test. B, Relative *CCL2, CCL5, ICAM-1, MMP-2,* and *MMP-9* mRNA expression levels normalized to 18S rRNA of VSMCs treated with rTW (100 ng/mL) or rTW plus rCD (0.01-0.5 µg/mL) during 24 hours. The same cDNA was repeatedly tested for multiple genes. Data represent the mean ± SEM of three independent experiments. *$P < .05$ vs Control; †$P < .05$ vs rTW. Student's *t* test. C, Effect of CD163 on CCL2 and CCL5 secretion induced by TWEAK in VSMCs. VSMCs were incubated with rTW (100 ng/mL) or rTW plus rCD (0.01-0.5 µg/mL) during 24 hours and supernatants were tested by ELISA for CCL2 or CCL5. Data represent the mean ± SEM of six independent experiments; *$P < .001$ vs control; †$P < .001$ vs rTW; Student's *t* test. D, Peritoneal macrophages were seeded in the upper surface of chemotaxis chambers and stimulated with the supernatants of VSMCs treated with 0% FBS (control), rTWEAK (100 ng/mL) or rTW plus rCD (0.1-0.5 µg/mL). Quantification of migrated cells in 10 fields per condition is shown in the right panel. Data represent the mean ± SEM of four independent experiments; *$P < .001$ vs Control; †$P < .001$ vs rTW; Student's *t* test. Scale bars, 50 µm

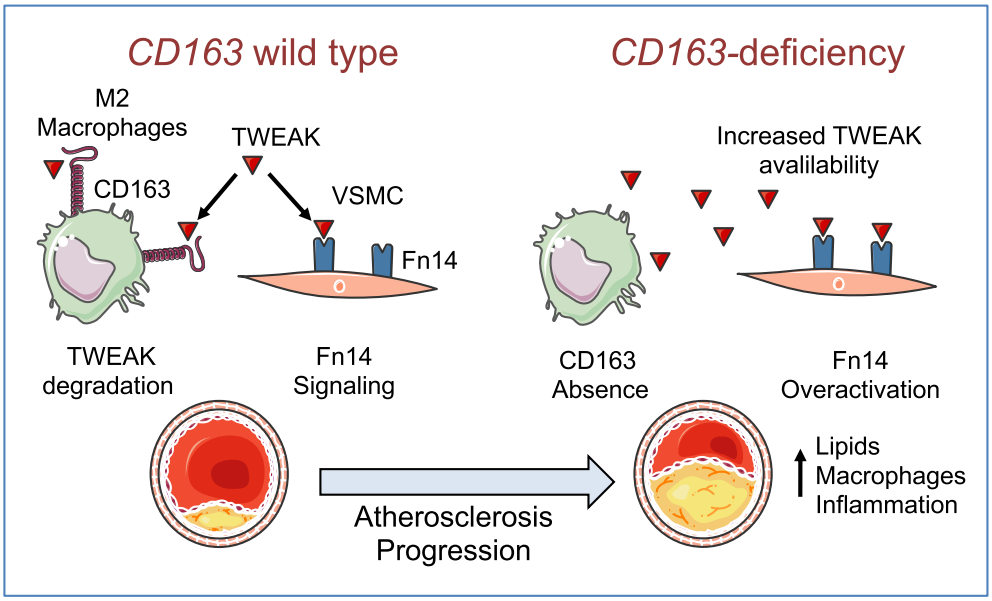

FIGURE 7 Model illustrating the potential mechanism of CD163. Cartoon depicting the role of CD163 as a receptor for TWEAK. In normal conditions, M2-type macrophages express CD163 and compete with Fn14 to bind TWEAK, limiting the pro-inflammatory effects of TWEAK/Fn14 interaction. However, absence of CD163 in macrophages increases TWEAK availability, favoring its interaction with Fn14, and promoting atherosclerosis progression

ApoE/CD163 double-deficient mice.[11] However, the mice used in the mentioned study are elderly (1-year old) and intraplaque hemorrhage is present in their BCA plaques. In this context, it is conceivable that Hb and TWEAK could compete to bind CD163 as demonstrated in vitro,[12] and that the M(Hb) macrophages display a pro-inflammatory phenotype due to an increase in TWEAK availability. However, CD163 is also expressed in early lesions from mice and humans in which intraplaque hemorrhage is absent[11,42] and its role in the progression of those lesions have not been previously assessed.

CD163 and TWEAK colocalize in both human carotid and femoral atherosclerotic plaques, suggesting a potential in vivo interaction.[36,40] Accordingly, CD163 can interact with TWEAK to regulate tissue regeneration after ischemic injury.[43] Now, our study demonstrates that CD163 could prevent the deleterious effects of TWEAK during the progression of atherosclerosis. $ApoE^{-/-}CD163^{-/-}$ mice injected with TWEAK showed a marked increase in the progression of atherosclerosis in both the aortic root and BCA by augmenting lesion size, lipid accumulation, and inflammation compared with $ApoE^{-/-}CD163^{+/+}$ mice. In addition, TWEAK-injected $ApoE^{-/-}CD163^{-/-}$ mice showed an increase in plaque instability represented by a larger necrotic core and a higher presence of buried caps and medial erosion in BCA than $ApoE^{-/-}CD163^{+/+}$ mice. When $ApoE^{-/-}CD163^{-/-}$ mice were pretreated with recombinant CD163, all the proatherogenic effects of TWEAK were inhibited indicating that CD163 can block TWEAK signaling in vivo.

The underlying protective role of CD163 could be related with at least two different mechanisms. First, we show that *CD163* deficiency promotes foam cell formation through increased uptake of modified lipoproteins. The uptake of ox-LDL occurs via different receptors such as CD36 and SR-A.[44] We demonstrated that CD36 is upregulated in absence of CD163, without modifying cholesterol efflux and the levels of the cellular transporters involved in this process. Accordingly, it has been previously shown that when macrophages are polarized to an alternative phenotype, they lose their ability to retain lipids inside.[37] In fact, CD163-expressing macrophages differentiated with IL-4 showed a diminished lipid uptake and differentiation of macrophages with Hb:Hp totally abolished foam cell formation.[37]

Second, Fn14 is upregulated by ox-LDL or pro-inflammatory cytokines in VSMCs[20,45] and, under those conditions, TWEAK activates NF-kB signaling and different cytokines expression.[15] Now, we demonstrated that CD163 can inhibit the pro-inflammatory response of TWEAK in VSMCs, indicating that CD163 and Fn14 compete to bind TWEAK. In addition, recombinant CD163 diminished migration of macrophages induced by supernatants from VSMCs stimulated with TWEAK.

In conclusion, loss of CD163 in mice results in an increased circulating TWEAK concentration that can accelerate atherosclerotic plaque progression through the increase in lipid content, inflammation, and plaque size (Figure 7). In addition, treatment of *CD163*-deficient mice with recombinant CD163 can ameliorate the pro-inflammatory and proatherogenic effects of TWEAK. Our results reveal

that CD163-expressing macrophages have a protective role during the progression of atherosclerosis.

ACKNOWLEDGMENTS

This work was supported by Fondo de Investigaciones Sanitarias, Instituto de Salud Carlos III (ISCiii/FEDER PI16/01419, PI19/00128) and Spanish Biomedical Research Centre in Diabetes and Associated Metabolic Disorders (CIBERDEM) and Cardiovascular Disease (CIBERCV), Spain.

CONFLICT OF INTEREST

The authors declare that they have no conflict of interest.

AUTHOR CONTRIBUTIONS

The study was conceived by J. Egido, J.L. Martín-Ventura, and L.M. Blanco-Colio. C. Gutiérrez-Muñoz, N. Méndez-Barbero, P. Quesada, C. Sastre, and V. Fernández-Laso performed the experiments. J.C. Escolá-Gil performed cholesterol efflux experiments. P. Svendsen and S.K. Moestrup generated CD163 deficient mice. C. Gutiérrez-Muñoz, N. Méndez-Barbero, and L.M. Blanco-Colio analyzed the obtained data. L.M. Blanco-Colio wrote the manuscript with contributions of N. Méndez-Barbero, J.L. Martín-Ventura, J. Egido, and S.K. Moestrup. All authors read and approved the manuscript.

REFERENCES

1. Swirski FK, Nahrendorf M. Leukocyte behavior in atherosclerosis, myocardial infarction, and heart failure. *Science*. 2013;339(6116):161-166.
2. Gordon S, Martinez FO. Alternative activation of macrophages: mechanism and functions. *Immunity*. 2010;32(5):593-604.
3. Gordon S. Alternative activation of macrophages. *Nat Rev Immunol*. 2003;3(1):23-35.
4. Pulford K, Micklem K, McCarthy S, Cordell J, Jones M, Mason DY. A monocyte/macrophage antigen recognized by the four antibodies GHI/61, Ber-MAC3, Ki-M8 and SM4. *Immunology*. 1992;75(4):588-595.
5. Kristiansen M, Graversen JH, Jacobsen C, et al. Identification of the haemoglobin scavenger receptor. *Nature*. 2001;409(6817):198-201.
6. Schaer CA, Schoedon G, Imhof A, Kurrer MO, Schaer DJ. Constitutive endocytosis of CD163 mediates hemoglobin-heme uptake and determines the noninflammatory and protective transcriptional response of macrophages to hemoglobin. *Circ Res*. 2006;99(9):943-950.
7. Etzerodt A, Maniecki MB, Møller K, Møller HJ, Moestrup SK. Tumor necrosis factor α-converting enzyme (TACE/ADAM17) mediates ectodomain shedding of the scavenger receptor CD163. *J Leukoc Biol*. 2010;88(6):1201-1205.
8. Timmermann M, Högger P. Oxidative stress and 8-iso-prostaglandin F(2alpha) induce ectodomain shedding of CD163 and release of tumor necrosis factor-alpha from human monocytes. *Free Radic Biol Med*. 2005;39(1):98-107.
9. Møller HJ. Soluble CD163. *Scand J Clin Lab Invest*. 2012;72(1):1-13.
10. Levy AP, Purushothaman KR, Levy NS, et al. Downregulation of the hemoglobin scavenger receptor in individuals with diabetes and the Hp 2–2 genotype: implications for the response to intraplaque hemorrhage and plaque vulnerability. *Circ Res*. 2007;101(1):106-110.
11. Guo L, Akahori H, Harari E, et al. CD163+ macrophages promote angiogenesis and vascular permeability accompanied by inflammation in atherosclerosis. *J Clin Invest*. 2018;128(3):1106-1124.
12. Bover LC, Cardó-Vila M, Kuniyasu A, et al. A previously unrecognized protein-protein interaction between TWEAK and CD163: potential biological implications. *J Immunol*. 2007;178(12):8183-8194.
13. Zheng TS, Burkly LC. No end in site: TWEAK/Fn14 activation and autoimmunity associated- end-organ pathologies. *J Leukoc Biol*. 2008;84(2):338-347.
14. Pamukcu B, Lip GYH, Shantsila E. The nuclear factor–kappa B pathway in atherosclerosis: a potential therapeutic target for atherothrombotic vascular disease. *Thromb Res*. 2011;128(2):117-123.
15. Winkles JA. The TWEAK-Fn14 cytokine-receptor axis: discovery, biology and therapeutic targeting. *Nat Rev Drug Discov*. 2008;7(5):411-425.
16. Bossen C, Ingold K, Tardivel A, et al. Interactions of tumor necrosis factor (TNF) and TNF receptor family members in the mouse and human. *J Biol Chem*. 2006;281(20):13964-13971.
17. Harada N, Nakayama M, Nakano H, Fukuchi Y, Yagita H, Okumura K. Pro-inflammatory effect of TWEAK/Fn14 interaction on human umbilical vein endothelial cells. *Biochem Biophys Res Commun*. 2002;299(3):488-493.
18. Lynch CN, Wang YC, Lund JK, Chen YW, Leal JA, Wiley SR. TWEAK induces angiogenesis and proliferation of endothelial cells. *J Biol Chem*. 1999;274(13):8455-8459.
19. Munoz-Garcia B, Madrigal-Matute J, Moreno JA, et al. TWEAK-Fn14 interaction enhances plasminogen activator inhibitor 1 and tissue factor expression in atherosclerotic plaques and in cultured vascular smooth muscle cells. *Cardiovasc Res*. 2011;89(1):225-233.
20. Munoz-Garcia B, Moreno JA, Lopez-Franco O, et al. Tumor necrosis factor-like weak inducer of apoptosis (TWEAK) enhances vascular and renal damage induced by hyperlipidemic diet in ApoE-knockout mice. *Arterioscler Thromb Vasc Biol*. 2009;29(12):2061-2068.
21. Schapira K, Burkly LC, Zheng TS, et al. Fn14-Fc fusion protein regulates atherosclerosis in ApoE-/- mice and inhibits macrophage lipid uptake in vitro. *Arterioscler Thromb Vasc Biol*. 2009;29(12):2021-2027.
22. Sastre C, Fernández-Laso V, Madrigal-Matute J, et al. Genetic deletion or TWEAK blocking antibody administration reduce atherosclerosis and enhance plaque stability in mice. *J Cell Mol Med*. 2014;18(4):721-734.
23. Stary HC, Chandler AB, Glagov S, et al. A definition of initial, fatty streak, and intermediate lesions of atherosclerosis. A report from the Committee on Vascular Lesions of the Council on Arteriosclerosis, American Heart Association. *Circulation*. 1994;89(5):2462-2478.
24. Tarín C, Fernández-Laso V, Sastre C, et al. Tumor necrosis factor-like weak inducer of apoptosis or Fn14 deficiency reduce elastase perfusion-induced aortic abdominal aneurysm in mice. *J Am Heart Assoc*. 2014;3(4):e000723.

25. Escola-Gil JC, Chen X, Julve J, et al. Hepatic lipase- and endothelial lipase-deficiency in mice promotes macrophage-to-feces RCT and HDL antioxidant properties. *Biochim Biophys Acta*. 2013;1831(4):691-697.
26. Rekhter MD. How to evaluate plaque vulnerability in animal models of atherosclerosis? *Cardiovasc Res*. 2002;54(1):36-41.
27. Rosenfeld ME, Polinsky P, Virmani R, Kauser K, Rubanyi G, Schwartz SM. Advanced atherosclerotic lesions in the innominate artery of the ApoE knockout mouse. *Arterioscler Thromb Vasc Biol*. 2000;20(12):2587-2592.
28. Stoll G, Bendszus M. Inflammation and atherosclerosis: novel insights into plaque formation and destabilization. *Stroke*. 2006;37(7):1923-1932.
29. Leitinger N, Schulman IG. Phenotypic polarization of macrophages in atherosclerosis. *Arterioscler Thromb Vasc Biol*. 2013;33(6):1120-1126.
30. Glass CK, Witztum JL. Atherosclerosis. The road ahead. *Cell*. 2001;104(4):503-516.
31. Buechler C, Ritter M, Orsó E, Langmann T, Klucken J, Schmitz G. Regulation of scavenger receptor CD163 expression in human monocytes and macrophages by pro- and antiinflammatory stimuli. *J Leukoc Biol*. 2000;67(1):97-103.
32. Blanco-Colio LM. TWEAK/Fn14 axis: a promising target for the treatment of cardiovascular diseases. *Front Immunol*. 2014;5:3.
33. Bouhlel MA, Derudas B, Rigamonti E, et al. PPARgamma activation primes human monocytes into alternative M2 macrophages with anti-inflammatory properties. *Cell Metab*. 2007;6(2):137-143.
34. Rahman K, Vengrenyuk Y, Ramsey SA, et al. Inflammatory Ly6Chi monocytes and their conversion to M2 macrophages drive atherosclerosis regression. *J Clin Invest*. 2017;127(8):2904-2915.
35. Møller HJ, Nielsen MJ, Maniecki MB, Madsen M, Moestrup SK. Soluble macrophage-derived CD163: a homogenous ectodomain protein with a dissociable haptoglobin-hemoglobin binding. *Immunobiology*. 2010;215(5):406-412.
36. Moreno JA, Dejouvencel T, Labreuche J, et al. Peripheral artery disease is associated with a high CD163/TWEAK plasma ratio. *Arterioscler Thromb Vasc Biol*. 2010;30(6):1253-1262.
37. Finn AV, Nakano M, Polavarapu R, et al. Hemoglobin directs macrophage differentiation and prevents foam cell formation in human atherosclerotic plaques. *J Am Coll Cardiol*. 2012;59(2):166-177.
38. Boyle JJ, Johns M, Kampfer T, et al. Activating transcription factor 1 directs Mhem atheroprotective macrophages through coordinated iron handling and foam cell protection. *Circ Res*. 2012;110(1):20-33.
39. Etzerodt A, Kjolby M, Nielsen MJ, Maniecki M, Svendsen P, Moestrup SK. Plasma clearance of hemoglobin and haptoglobin in mice and effect of CD163 gene targeting disruption. *Antioxid Redox Signal*. 2013;18(17):2254-2263.
40. Moreno JA, Munoz-Garcia B, Martín-Ventura JL, et al. The CD163-expressing macrophages recognize and internalize TWEAK: potential consequences in atherosclerosis. *Atherosclerosis*. 2009;207(1):103-110.
41. Libby P, Theroux P. Pathophysiology of coronary artery disease. *Circulation*. 2005;111(25):3481-3488.
42. Tarín C, Carril M, Martin-Ventura JL, et al. Targeted gold-coated iron oxide nanoparticles for CD163 detection in atherosclerosis by MRI. *Sci Rep*. 2015;5:17135.
43. Akahori H, Karmali V, Polavarapu R, et al. CD163 interacts with TWEAK to regulate tissue regeneration after ischaemic injury. *Nat Commun*. 2015;6:7792.
44. Greaves DR, Gordon S. The macrophage scavenger receptor at 30 years of age: current knowledge and future challenges. *J Lipid Res*. 2009;50(Suppl):S282-S286.
45. Munoz-Garcia B, Martin-Ventura JL, Martínez E, et al. Fn14 is upregulated in cytokine-stimulated vascular smooth muscle cells and is expressed in human carotid atherosclerotic plaques: modulation by atorvastatin. *Stroke*. 2006;37(8):2044-2053.

SUPPORTING INFORMATION

Additional Supporting Information may be found online in the Supporting Information section.

How to cite this article: Gutiérrez-Muñoz C, Méndez-Barbero N, Svendsen P, et al. CD163 deficiency increases foam cell formation and plaque progression in atherosclerotic mice. *The FASEB Journal*. 2020;34:14960–14976. https://doi.org/10.1096/fj.202000177R